Assignment 2: Eigenvalue Problems I

Marta Casado Carrasquer

April 8, 2025

1 Introduction

In this report we aim to solve an Eigenvalue Problem. The quantum harmonic oscillator problem has well-known analytical solutions for both eigenvalues and eigenfunctions. Hence, we focus on numerically solving the one-dimensional time-independent Schrödinger equation for the harmonic oscillator potential using finite difference methods. After constructing the Hamiltonian in dimensionless units, eigenvalues and eigenfunctions are computed using both direct diagonalization and inverse power iteration. The numerical scheme is validated against analytical results.

Furthermore, the scheme is extended to study the effects of a perturbed potential.

2 Theory and Methods

2.1 Problem Description

The objective is to numerically solve the one-dimensional eigenvalue problem:

$$H\Psi = E\Psi,$$

where

$$H = -\frac{\hbar^2}{2m}\frac{\partial^2}{\partial x^2} + V(x).$$

and $V(x) = \frac{1}{2}m\omega^2 x^2$ is the harmonic oscillator potential. To simplify the problem, the Hamiltonian is transformed into dimensionless units.

2.2 Dimensionless Hamiltonian

We introduce a dimensionless spatial variable z, defined as:

$$z = x\sqrt{\frac{m\omega}{\hbar}},$$

where $\hbar$ is the reduced Planck constant, m is the particle mass, and ω is the angular frequency of the harmonic oscillator. Using this substitution, the second derivative transforms as:

$$\frac{\partial^2}{\partial x^2} = \frac{m\omega}{\hbar}\frac{\partial^2}{\partial z^2}.$$

The Hamiltonian in dimensionless units becomes:

$$H = \frac{\hbar\omega}{2}\left(-\frac{\partial^2}{\partial z^2} + z^2\right).$$

Rewriting the Schrödinger equation:

$$\frac{1}{2}\left(-\frac{\partial^2}{\partial z^2} + z^2\right)\Psi = \frac{E}{\hbar\omega}\Psi,$$

we see that the eigenvalues E are expressed in units of $\hbar\omega$, making the problem dimensionless and simplifying numerical computations.

2.3 Numerical Discretization

The spatial domain $z \in [z_{\min}, z_{\max}]$ is divided into N equally spaced intervals:

$$z_i = z_{\min} + i\Delta z, \quad i = 0, 1, \ldots, N,$$

where $\Delta z = \frac{z_{\max} - z_{\min}}{N}$ is the grid spacing. The wavefunction $\Psi(z)$ is approximated at the grid points z_i, and the potential $V(z)$ is evaluated at these points.

2.4 Finite Difference Approach

The kinetic energy term is discretized using finite difference methods:

- **Three-point stencil:**

$$\Psi''(z) \approx \frac{\Psi(z + \Delta z) - 2\Psi(z) + \Psi(z - \Delta z)}{(\Delta z)^2}.$$

- **Five-point stencil:**

$$\Psi''(z) \approx \frac{-\Psi(z-2\Delta z) + 16\Psi(z-\Delta z) - 30\Psi(z) + 16\Psi(z+\Delta z) - \Psi(z+2\Delta z)}{12(\Delta z)^2}.$$

The Hamiltonian matrix H is then constructed as:

$$H = -\frac{1}{2}A + \text{diag}(V),$$

$$H = -\frac{1}{2}B + \text{diag}(V),$$

where A or B are the finite difference coefficient matrices derived using the chosen stencil and V is the potential added to the diagonal.

2.5 Perturbed Potential

Once we have solved for a known case, a perturbed potential with a Gaussian "bump" is analysed. We modify the potential as follows:

$$V_{bump}(z) = \frac{z^2}{2} + C_1 e^{(-C_2 z^2)},$$

where C_1 and C_2 are constants that control the height and width of the perturbation, respectively.

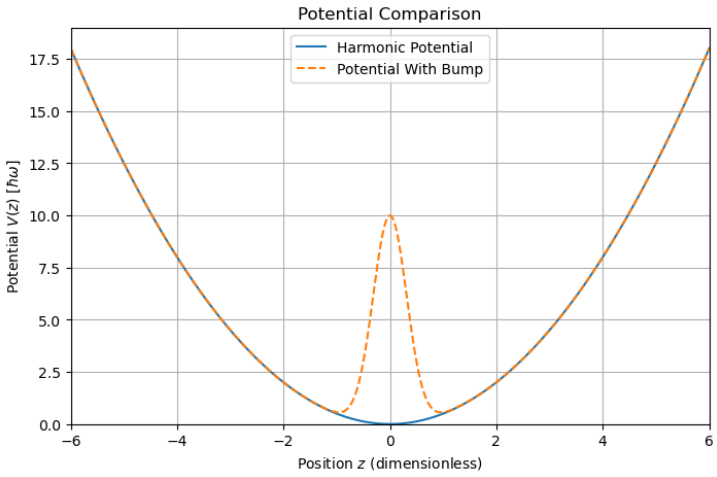

Figure 1: Perturbed potential with $C_1 = 10$ and $C_2 = 5$ plotted in comparison with the Harmonic potential.

2.6 Eigenvalue Problem

The matrix eigenvalue problem $H\Psi = E\Psi$ is solved using the following methods:

2.6.1 Direct Diagonalization:

The `eigh` routine from `scipy.linalg` in Python is used to compute all eigenvalues and eigenvectors of H.

2.6.2 Inverse Power Iteration with Shift:

Given the Hamiltonian matrix H, we aim to find its smallest eigenvalue $\lambda_{\min}$. Instead of directly solving the eigenvalue equation $H\Psi = \lambda\Psi$, we use an iterative approach by solving the shifted equation:

$$(H - \xi I)\Psi = \nu\Psi,$$

where ξ is a chosen shift, I is the identity matrix, and ν is the eigenvalue of the shifted Hamiltonian $H_{\text{shifted}} = H - \xi I$.

The algorithm is implemented as follows:

1. **LU Factorization:** To efficiently solve the linear system $(H_{\text{shifted}})y = b$ at each iteration, H_{shifted} is decomposed into its lower and upper triangular matrices L and U:

$$H_{\text{shifted}} = LU.$$

2. **Initialization:** The algorithm begins with a randomly initialized vector y_0, which is normalized:

$$y_0 = \frac{y_0}{\|y_0\|}.$$

3. **Iterative Update:** For each iteration k, we proceed as follows:

   (a) Solve the linear system $H_{\text{shifted}}y_{k+1} = y_k$ using the LU decomposition:

$$y_{k+1} = (H_{\text{shifted}})^{-1}y_k.$$

   (b) Normalize y_{k+1} to avoid numerical instability:

$$y_{k+1} = \frac{y_{k+1}}{\|y_{k+1}\|}.$$

4. **Eigenvalue Estimation:** At each iteration, the eigenvalue ν is estimated using the quotient:

$$\nu = \frac{y_k^\dagger y_{k+1}}{y_k^\dagger y_k},$$

where $y_k^\dagger$ denotes the Hermitian transpose. The original eigenvalue is computed as:

$$\lambda = \xi + \frac{1}{\nu}.$$

5. **Convergence Criterion:** The iteration continues until the difference between successive eigenvectors satisfies:

$$\|y_{k+1} - y_k\| < \epsilon,$$

where ϵ is a predefined tolerance.

3 Results and Discussions

3.1 Discretization and Choice of Parameters

To numerically solve our problem, the spatial domain $[-6, 6]$ was discretized into $N = 400$ intervals. This value was chosen after testing showed that it provided better results for higher-order eigenvalues. A larger domain choice, e.g. $[-10, 10]$ was inefficient since the solutions for the eigenfunctions at those points gave 0.

We also note that only the interior points of the domain were used to build the finite-difference Hamiltonian.

3.2 Finite Difference Stencil and Matrix Properties

Although both three-point and five-point finite difference stencils were implemented, calculations were performed using the five-point stencil due to its improved accuracy in approximating the second derivative.

Different matrix properties were checked to ensure its correctness.

The matrix H was verified to be real and symmetric:

- `np.all(np.isreal(H))` $\Rightarrow$ `True`
- `np.allclose(H, H.T)` $\Rightarrow$ `True`

Furthermore, orthogonality of the eigenvectors was confirmed numerically by checking the dot product between different eigenvectors and by computing $V^\top V$, where V is the matrix of eigenvectors.

3.3 Eigenvalue Problem with `eigh`

The eigenvalues and eigenvectors of the Hamiltonian were obtained using the `scipy.linalg.eigh` routine. The first five eigenvalues computed numerically are:

n	Numerical Eigenvalue
0	0.499999992
1	1.49999994
2	2.49999979
3	3.49999947
4	4.49999891

These numerical values closely match the analytical eigenvalues of the harmonic oscillator, $E_n = n + \frac{1}{2}$.

Plots of the corresponding eigenfunctions are shown below:

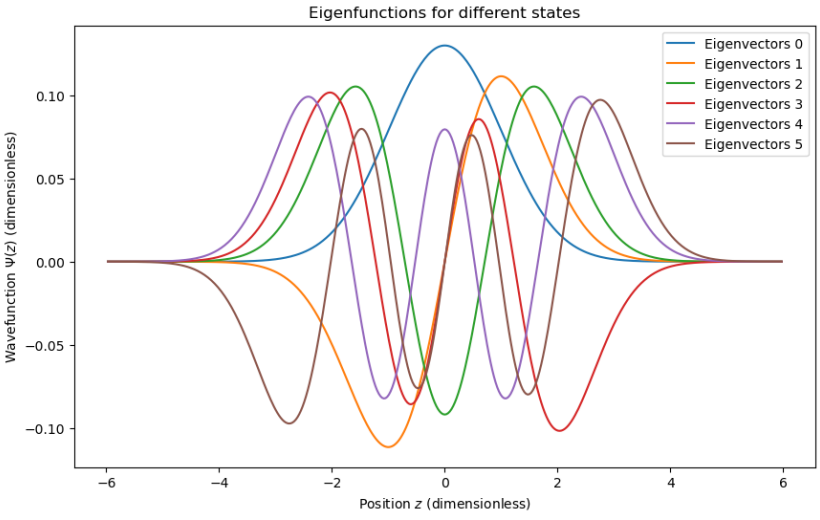

Figure 2: Plot for the first five eigenfunctions.

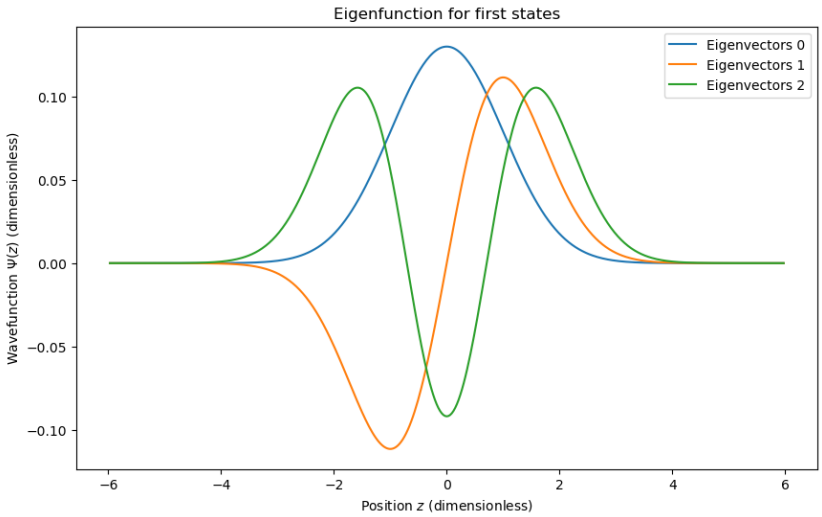

Figure 3: Plot for the first three eigenfunctions.

3.4 Inverse Power Iteration with Shift

We can compute a specific eigenvalue with the inverse power iteration method. For instance, to obtain the third order eigenvalue we use a shift $\xi = 2.25$ and $\xi = 2.00$. The method converges faster when the shift is close to the actual eigenvalue. Figure 4 and Figure 5, show the plotted eigenvector for different number of iterations:

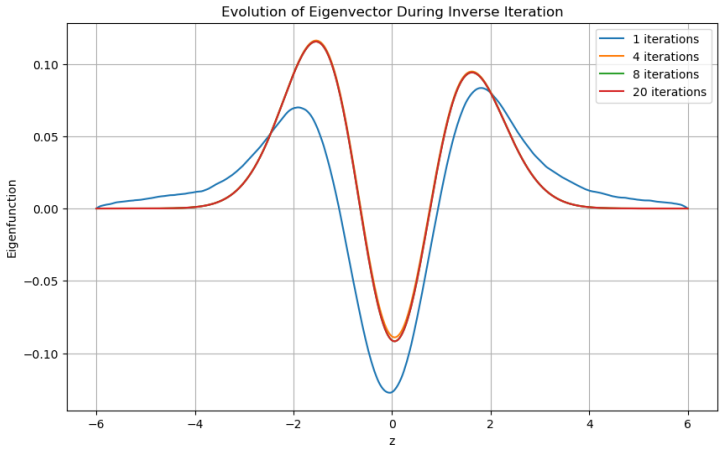

Figure 4: Evolution of the eigenvector for $\xi = 2.00$ during inverse power iteration.

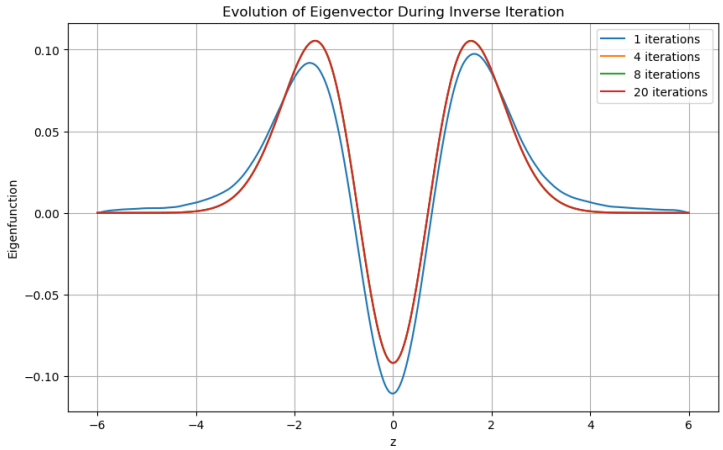

Figure 5: Evolution of the eigenvector for $\xi = 2.25$ during inverse power iteration.

Additionally, Figure 6 and Figure 7 display the convergence behaviour of the estimated eigenvalue.

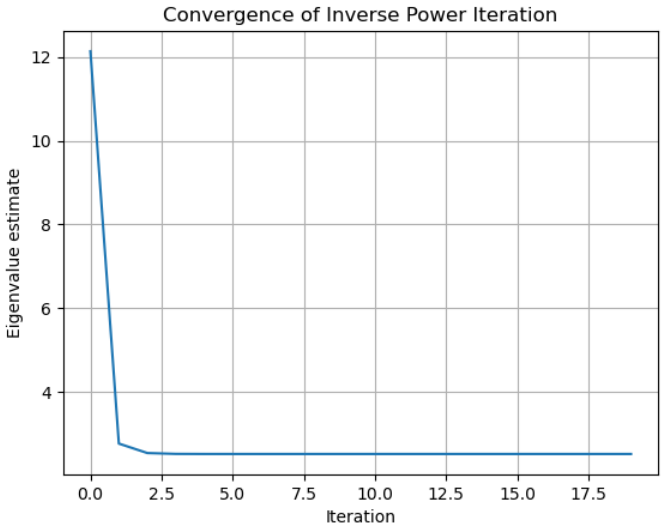

Figure 6: Convergence of the eigenvalue estimate for $\xi = 2.00$ during inverse iteration.

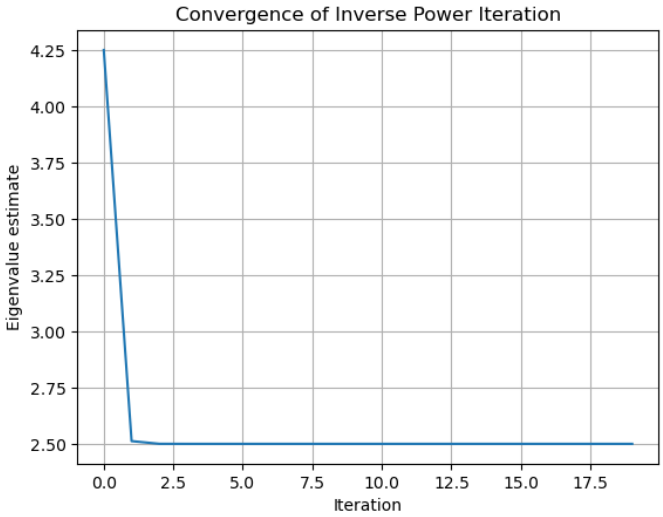

Figure 7: Convergence of the eigenvalue estimate for $\xi = 2.25$ during inverse iteration.

3.5 Effect of the Perturbed Potential

To explore quantum tunnelling behaviour we introduce $V_{\text{bump}}(z)$ as mention in the previous section. Several choices of C_1 and C_2 were made. We shall now discuss for $C_1 = 10$ and $C_2 = 5$ by looking at Figure 8.

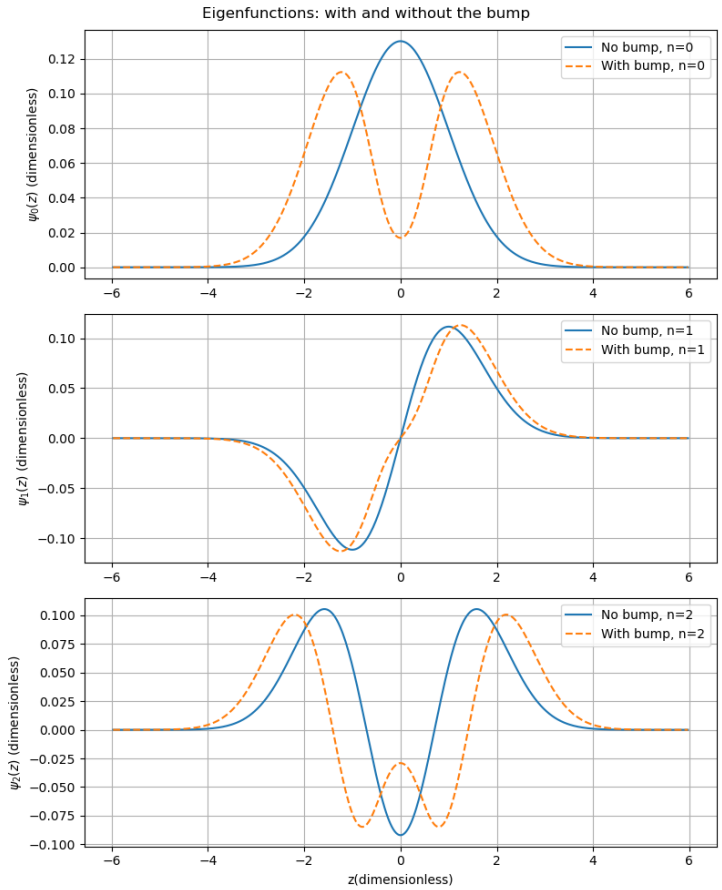

Figure 8: Comparison of eigenfunctions with and without the central bump in the potential.

The plot shows the first three eigenfunctions (for $n = 0, 1, 2$) for the standard harmonic oscillator and the modified potential.

Ground State ($n = 0$):

- The eigenfunction with the bump has two clear peaks, one on each side of $x = 0$, suggesting that the wavefunction is split across the barrier — an indication of quantum tunneling.

First Excited State ($n = 1$):

- The node structure is similar to the unperturbed one, but the antisymmetric shape becomes more pronounced due to the bump.

- The eigenfunction still shows tunnelling behaviour, but it is now more localized on one side.

Second Excited State ($n = 2$):

- The wavefunction has three peaks.
- The bump still alters the node structure, but its effect is not as intense compared to the lower energy states.

3.6 Comparison with Analytical Solutions

In order to validate the accuracy of our numerical method, we make a comparison with the known analytical results.

For the harmonic oscillator, the analytical eigenvalues are given by:

$$E_n^{(\text{analytical})} = n + \frac{1}{2}.$$

The following plot, compares the analytical eigenvalues with the ones solved numerically

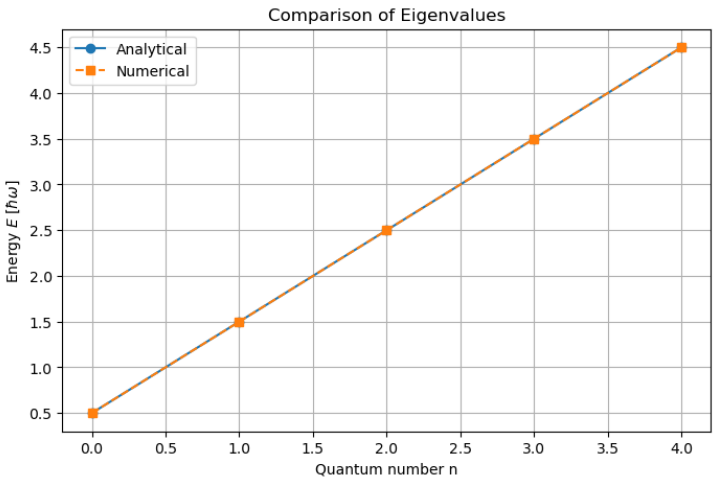

Figure 9: Comparison of numerical and analytical eigenvalues for the harmonic oscillator.

Moreover, the eigenfunctions were compared to the analytical forms:

$$\psi_n(x) = N_n H_n(x) e^{-x^2/2},$$

where $H_n(x)$ are Hermite polynomials. Figure 10 shows perfect agreement in both amplitude and shape between the numerical and analytical solutions for the first eigenfunction $n = 0$.

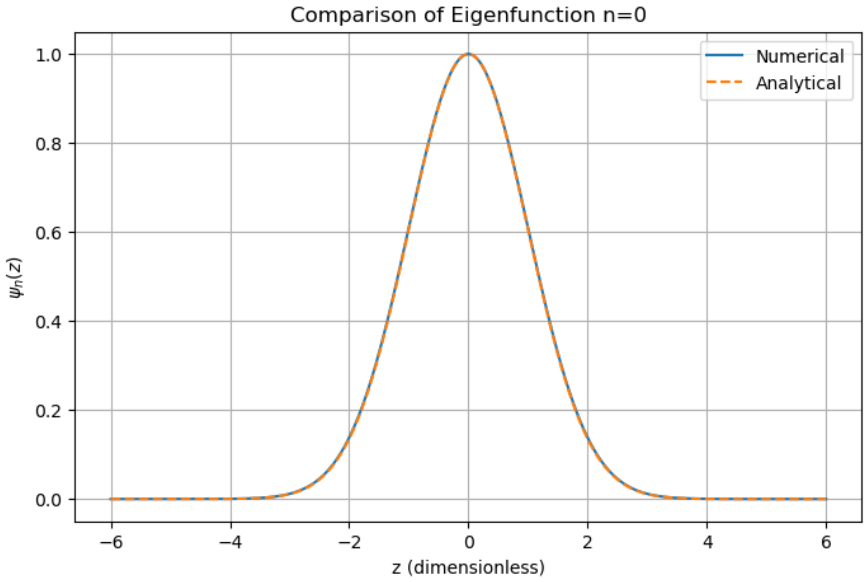

Figure 10: Comparison of numerical and analytical eigenfunctions for the harmonic oscillator.

Finally, a convergence plot is shown with varying $N = 50, 100, 200, 400$. The maximum error decreases consistently with increasing N, as shown in Figure 11. This confirms the consistency and reliability of the numerical scheme.

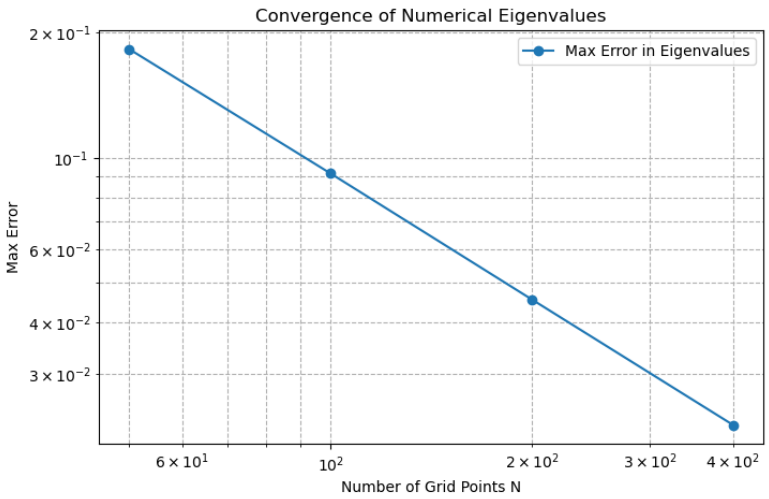

Figure 11: Convergence of eigenvalue error with increasing number of grid points.

3.7 Numerical Error

There are two main sources of error in this numerical approach:

1. **Finite Difference Approximation:** While the five-point stencil significantly reduces the discretization error compared to the three-point stencil, the method still introduces an $\mathcal{O}(\Delta z^4)$ error in the second derivative.

2. **Boundary Conditions:** The wavefunction is enforced to vanish at the boundaries of the grid. This Dirichlet boundary conditions at $x = \pm 6$, modifying the true infinite potential well scenario and introduce a boundary error.

4 Conclusions

The numerical methods implemented yield accurate results for the quantum harmonic oscillator. Including a central bump in the potential allows us to explore tunnelling phenomena. Comparisons with analytical solutions confirm the validity of the numerical approach.